

MAJOR PAPER

Additive Value of 3T 3D CISS Imaging to Conventional MRI for Assessing the Abnormal Vessels of Spinal Dural Arteriovenous Fistulae

Hiroyuki Uetani^{1*}, Toshinori Hirai², Mika Kitajima¹, Minako Azuma²,
Shigetoshi Yano³, Hideo Nakamura³, Keishi Makino³, Yutaka Kai⁴,
Yasunori Nagayama¹, Yoshihito Kadota², and Yasuyuki Yamashita¹

Introduction: We investigated the additive value of the 3T 3D constructive interference in steady state (CISS) sequence to conventional MRI for the evaluation of spinal dural arteriovenous fistulae (SDAVF).

Materials and Methods: We included 16 consecutive patients (15 men, 1 woman; age range 42–81 years; mean 64 years) with SDAVF who underwent 3T MRI and digital subtraction angiography (DSA) before treatment. Two neuroradiologists independently evaluated the presence of abnormal vessels on 3D CISS-, T₂- and T₁-weighted images (T₁WI, T₂WI), and contrast-enhanced T₁WI using a 3-point grading system. Interobserver agreement was assessed by calculating the κ coefficient.

Results: The SDAVF site was the cervical region in one patient, the thoracic region in 12 patients, the lumbar region in two, and the sacral region in one. For the visualization of abnormal vessels, the mean score was significantly higher for 3D CISS than the other sequences ($P < 0.05$). In 12 of 16 cases (75%) both readers made definite positive findings on additional 3D-CISS images. Interobserver agreement was excellent for 3D CISS images ($\kappa = 1.0$), good for T₁WI ($\kappa = 0.78$; 95% confidence interval [CI] 0.54–1.00) and T₂WI ($\kappa = 0.74$; 95% CI 0.48–1.00) and moderate for contrast-enhanced T₁WI (CET₁WI) ($\kappa = 0.50$; 95% CI 0.21–0.80).

Conclusion: For the assessment of abnormal vessels of SDAVF, the 3T 3D CISS sequence adds value to conventional MRI.

Keywords: *spinal dural arteriovenous fistulae, constructive interference in steady state, magnetic resonance imaging, arteriovenous fistulae, abnormal vessels*

Introduction

Spinal dural arteriovenous fistulae (SDAVF) have been underdiagnosed. If not treated adequately, they can lead to considerable morbidity with progressive spinal cord symptoms.¹ SDAVF are predominantly seen in elderly men.² Initially, the symptoms and signs of SDAVF can mimic degenerative spine disease or infectious or transverse myelopathy. The symptoms

can persist for several months before a correct diagnosis is made.³ MRI usually exhibits characteristic findings of intramedullary T₂ hyperintensity, variable intramedullary and leptomeningeal enhancement, a mild to moderate mass effect, and tortuous, exuberant vascular flow voids along the dorsal spinal cord, primarily involving the thoracic spinal cord and conus medullaris.^{1,4} Tortuous and exuberant vessels were seen in 35–91% of patients on conventional MRI, i.e., T₂- and T₁-weighted images (T₁WI, T₂WI), and on contrast-enhanced T₁WI (CET₁WI).^{2,4,5} However, if the shunt volume is small, they might not be seen on conventional sequences.

In the evaluation of SDAVF, coiled or serpentine vascular structures may be better appreciated on heavily T₂-weighted than on standard T₂ turbo-spin echo sequences.^{6,7} The constructive interference in steady state (CISS) sequence can yield high-resolution images with good contrast between cerebrospinal fluid (CSF) and intradural vessels.⁶

While there are a few case reports documenting the usefulness of CISS sequences for the identification of abnormal vessels of SDAVF,^{1,6,8} the additive value of 3D CISS imaging

¹Department of Diagnostic Radiology, Graduate School of Medical Sciences, Kumamoto University, 1-1-1 Honjo, Chuo-ku, Kumamoto, Kumamoto 860-8556, Japan

²Department of Radiology, Faculty of Medicine, Miyazaki University, Miyazaki, Japan

³Department of Diagnostic Neurosurgery, Graduate School of Medical Sciences, Kumamoto University, Kumamoto, Japan

⁴Department of Neurosurgery, Aso Central Hospital, Kumamoto, Japan

*Corresponding author, Phone: +81-96-373-5261, Fax: +81-96-362-4330, E-mail: hama-moto@hotmail.co.jp

©2017 Japanese Society for Magnetic Resonance in Medicine

This work is licensed under a Creative Commons Attribution-NonCommercial-NoDerivatives International License.

to conventional MRI for the evaluation of SDAVF has not been systematically investigated. The purpose of this study was to assess the additive value of 3T 3D-CISS imaging to conventional MRI for the evaluation of the abnormal vessels of SDAVF.

Materials and Methods

Study population and MR technique

We declare that all human studies have been approved by the Kumamoto University Hospital ethics committee and have therefore been performed in accordance with the ethical standards laid down in the 1964 Declaration of Helsinki and its later amendments. This retrospective study was approved by the ethics committee, and informed consent was waived. We retrospectively assessed 16 consecutive patients with SDAVF diagnosed on digital subtraction angiography (DSA) at Kumamoto University Hospital. They were 15 men and 1 woman ranging in age from 42 to 81 years (mean 64 years). All scans were acquired on a 3T MR unit (Magnetom Trio; Siemens, Erlangen, Germany) with a spinal matrix coil; DSA was performed preoperatively. We examined sagittal slabs on the 3D CISS sequences and conventional sagittal and axial 2D-T₁WI, T₂WI, and CET₁WI. All images were acquired with a rectangular FOV to obtain finer spatial resolution in the phase-encoding direction.

The parameters we used were: Sagittal T₁W spin-echo (SE) sequences, TR/TE 600/8.6 ms, 1 excitation, section thickness 3 mm, intersection gap 0.3 mm, FOV 280 × 280 mm, matrix 224 × 320, acquisition time = 2 min 54 s; axial T₁W SE sequences, TR/TE_{eff} 600/10 ms, 1 excitation, section thickness 3 or 4 mm, intersection gap 0.3 mm, FOV 180 × 180 mm, acquisition time = 3 min 12 s; sagittal T₂W fast SE (FSE) sequence, TR/TE_{eff} 3000/70 ms, 1 excitation, section thickness 3 mm, intersection gap 0.3 mm, FOV 280 × 280 mm, matrix 269 × 384, acquisition time = 2 min 16 s; axial T₂W FSE sequences, TR/TE_{eff} 4000/70 ms, 1 excitation, section thickness 3 or 4 mm, intersection gap 0.3 mm, FOV 180 × 180 mm, acquisition time = 2 min 24 s; CISS sequence, TR/TE 7.1/2.8 ms, 1 excitation, section thickness 0.5 mm, flip angle 43°, FOV 250 mm, matrix 256 × 512, slab thickness = 32 mm, acquisition time = 3 min 43 s.

The sagittal and axial contrast-enhanced T₁W SE sequences were acquired with the same parameters as the precontrast MRI scans and the oblique coronal reconstruction CISS images were created with a multiplanar reconstruction technique.

DSA technique

Diagnostic intra-arterial DSA via a femoral arterial approach was performed in a biplane angiography suite (Allura Xper FD; Philips Healthcare, Best, the Netherlands) by a trained neuroradiologist and/or a neurosurgeon. The angiographic technique included the selective manual injection of 3–5 ml of a 300-mg/ml iodinated nonionic

contrast agent into the intended arteries and anteroposterior imaging at a rate of 3 frames/s. The matrix was 2048 × 2048 and the FOV was 42 cm.

To obtain 3D images of the vessels injected from the feeder and of the bony structures, we acquired 3D rotational angiographs on the same angiography system. On a dedicated commercially available workstation (Philips Healthcare) we then reconstructed and analyzed the filling run-volume. The 3D images were reconstructed in a 512 × 512 × 512 matrix with an isotropic voxel size.

Image evaluation

Two readers with 23 and 21 years of experience in neuroangiography consensually evaluated the entire series of DSA images on a picture archiving and communication system (PACS) workstation. Two other observers with 19 and 18 years of experience in diagnostic neuro-MRI who were blinded to clinical information and DSA results independently evaluated the presence of abnormal vessels on 3D CISS images and T₂WI, T₁WI, and CET₁WI on a PACS workstation. They used a 3-point grading system where grade 3 = definitely positive, grade 2 = probably positive, and grade 1 = equivocal or definitely negative. First, the readers analyzed conventional sequences (T₁WI, T₂WI, and CET₁WI), and the 3D CISS images were analyzed 2 weeks later without conventional sequences.

Statistical analysis

We used κ coefficient to assess the interobserver agreement in each type of sequence; $\kappa < 0.20$ = poor, 0.21–0.40 = fair, 0.41–0.60 = moderate, 0.61–0.80 = good, 0.81–0.90 = very good, and $\kappa > 0.90$ = excellent. The Friedman test and the Scheffe test were used to evaluate the grading differences of the four types of images. Differences of $P < 0.05$ were considered to indicate a statistically significant difference.

Results

Tables 1 and 2 shows the summary of clinical findings, MR findings, and grade assessment for the 4 MR sequences in 16 patients with SDAVF. DSA confirmed that the fistulae were located in the cervical region in one-, the thoracic region in 12-, the lumbar region in 2-, and the sacral region in one patient. For the presence of abnormal vessels, 2 readers assigned grade 3 to all 3D CISS images and grade 1 to 14 cases on T₁WI. On T₂WI, reader 1 assigned grade 3 to 3-, grade 2 to 10-, and grade 1 to 3 cases. Reader 2 recorded as grade 3 in 4-, grade 2 in 7-, and grade 1 in 5 cases. On CET₁WI scans reader 1 scored 3 cases as grade 3, 6 as grade 2, and 7 as grade 1; reader 2 judged one case as grade 3, 4 as grade 2, and 11 as grade 1.

Interobserver agreement was excellent for 3D CISS images ($\kappa = 1.0$), good for T₁WI ($\kappa = 0.78$; 95% confidence interval [CI] 0.54–1.00) and T₂WI ($\kappa = 0.74$; 95% CI 0.48–1.00) and moderate for CET₁WI ($\kappa = 0.50$; 95% CI 0.21–0.80).

Table 1. Summary of 16 patients with spinal dural arteriovenous fistulae

Case/Age (year)/Sex	Symptoms						Time from onset to diagnosis (months)
	Paresthesias	Leg weakness	Disturbances in sensation	Pain	Disturbances in gait		
1/58/M	-	+	+	+	-	3	
2/75/M	-	+	+	-	+	4	
3/60/M	-	+	-	+	+	3	
4/58/M	+	+	+	-	+	12	
5/73/M	-	+	+	-	-	8	
6/75/F	-	+	-	-	+	6	
7/62/M	+	+	+	-	-	28	
8/78/M	-	+	-	-	-	9	
9/58/M	-	+	-	-	-	7	
10/52/M	-	-	-	-	-	13	
11/78/M	+	+	+	+	+	6	
12/59/M	+	+	-	-	+	10	
13/81/M	-	+	+	-	+	4	
14/42/M	-	+	+	-	+	13	
15/56/M	+	+	-	-	+	20	
16/63/M	+	+	+	-	+	16	

M, male; F, female.

Table 2. Summary of MR abnormalities and grade assessment for 4 MR sequences in 16 patients with spinal dural arteriovenous fistulae

Case	Extent of intramedullary T ₂ hyperintensity	Fistula site	Feeder	T ₂ WI		T ₁ WI		CET ₁ WI		CISS	
				R1	R2	R1	R2	R1	R2	R1	R2
1	T3–8	T5	Intercostal a.	3	3	1	1	3	3	3	3
2	T7–conus	T6	Intercostal a.	2	2	1	1	2	1	3	3
3	T8–conus	T7	Intercostal a.	2	1	1	1	2	1	3	3
4	T4–conus	T7	Intercostal a.	2	2	1	1	2	1	3	3
5	T8–12	T7	Intercostal a.	3	3	1	1	1	1	3	3
6	T8–11	T9	Intercostal a.	2	1	1	1	1	1	3	3
7	T5–conus	T10	Intercostal a.	2	2	1	1	1	1	3	3
8	T7–11	T10	Intercostal a.	1	1	1	1	1	1	3	3
9	T5–conus	L3	Lumbar a.	1	1	1	1	1	1	3	3
10	none	C5	Vertebral a.	2	2	1	1	3	2	3	3
11	T1–10	T2	Intercostal a.	1	1	1	1	1	1	3	3
12	T4–conus	L1	Lumbar a.	2	2	1	1	2	2	3	3
13	T5–conus	T7	Intercostal a.	2	2	1	1	1	1	3	3
14	T6–conus	T6	Intercostal a.	2	3	2	2	2	2	3	3
15	T7–conus	S2	Iliolumbar a.	3	3	3	2	3	2	3	3
16	T7–conus	T11	Intercostal a.	2	2	1	1	2	1	3	3

The presence of abnormal vessels on each sequence was qualitatively evaluated using a 3-point grading system: 3, definitely positive; 2, probably positive; 1, equivocal or definitely negative. C, Cervical; CET₁WI, contrast-enhanced T₁-weighted imaging; CISS, constructive interference in steady state imaging; L, Lumbar; R1, reader 1; R2, reader 2; S, Sacral; T, thoracic; T₁WI, T₁-weighted imaging; T₂WI, T₂-weighted imaging.

Table 3 shows the comparative result of the mean score of the 4 MR sequences. There were statistical significant differences in mean score among 4 MR sequences ($P < 0.001$). The mean scores were significantly higher for 3D CISS than T_2 WI, T_1 WI, and CET_1 WI ($P < 0.05$). There were no statistical significant differences in the mean score among T_2 WI, T_1 WI, and CET_1 WI.

In 12 of 16 cases (75%) both readers reported definite positive findings when 3D CISS images were added (Fig. 1). After the addition of 3D CISS imaging, the judgment of reader 1 changed from grade 1 to grade 3 in 3 (19%) and from grade 2 to grade 3 in 9 (56%) cases. For reader 2 the change was from grade 1 to grade 3 in 5 (31%) and from grade 2 to grade 3 in 7 (44%) cases.

Discussion

We found that 3D CISS imaging had additive values to conventional MRI for demonstrating the abnormal vessels of SDAVF. We attribute the superiority of the 3D CISS technique over the

other sequences to its providing the higher spatial resolution essential for the delineation of the abnormal vessels within the CSF. In contrast to submillimeter sections without intersection gaps on 3D CISS sequences, on SE sequences the section thickness and the intersection gaps are usually 3- or 4 mm. The contiguous thin-slice sections on 3D CISS images facilitated the detection of the detailed structure and extent of the abnormal vessels. Also, the 3D CISS sequence yields better contrast between the CSF and solid structures including the spinal cord, dura mater, nerve roots, and venous structures⁹ and there are significantly fewer CSF flow artifacts. According to Haacke et al.,¹⁰ 3D CISS sequence yields fewer flow artifact than other sequences (e.g. FSE and other gradient-echo techniques) by summing steady state precession fast imaging with steady state precession (FISP) with an alternating-, and reversed FISP (PSIF) with a non-alternating radiofrequency pulse.

Spinal DSA is the diagnostic gold standard for SDAVF; it offers the additional advantage of possible simultaneous treatment, but it is invasive and time-consuming. MRI often suggests the diagnosis non-invasively. MRI findings with the highest sensitivity for SDAVF included intramedullary T_2 hyperintensity and exuberant and tortuous vessels on either the ventral or the dorsal side of the spinal cord. The specificity of flow voids, but not of T_2 hyperintensity, was very high for spinal AVF.¹¹ Gilbertson et al.⁴ found flow voids on 35% of T_1 WI- and on 45% of T_2 WI scans and Hurst and Grossman⁵ detected flow voids on 91% of T_2 WI- and 70% of CET_1 WI scans. Based on their literature review, Toossi et al.¹¹ concluded that flow voids were found on 89% of MRI scans of

Table 3. Comparison of the mean score of the 4 MR sequences

	T_1 WI	T_2 WI	CET_1 WI	CISS
Reader 1	1.2 ± 0.5	2.0 ± 0.6	1.8 ± 0.8	3.0 ± 0.0*
Reader 2	1.1 ± 0.3	1.9 ± 0.8	1.4 ± 0.6	3.0 ± 0.0*

*The mean score was significantly higher for CISS than the other sequences ($P < 0.05$). CET_1 WI, contrast-enhanced T_1 -weighted imaging; CISS, constructive interference in steady state imaging; T_1 WI, T_1 -weighted imaging; T_2 WI, T_2 -weighted imaging.

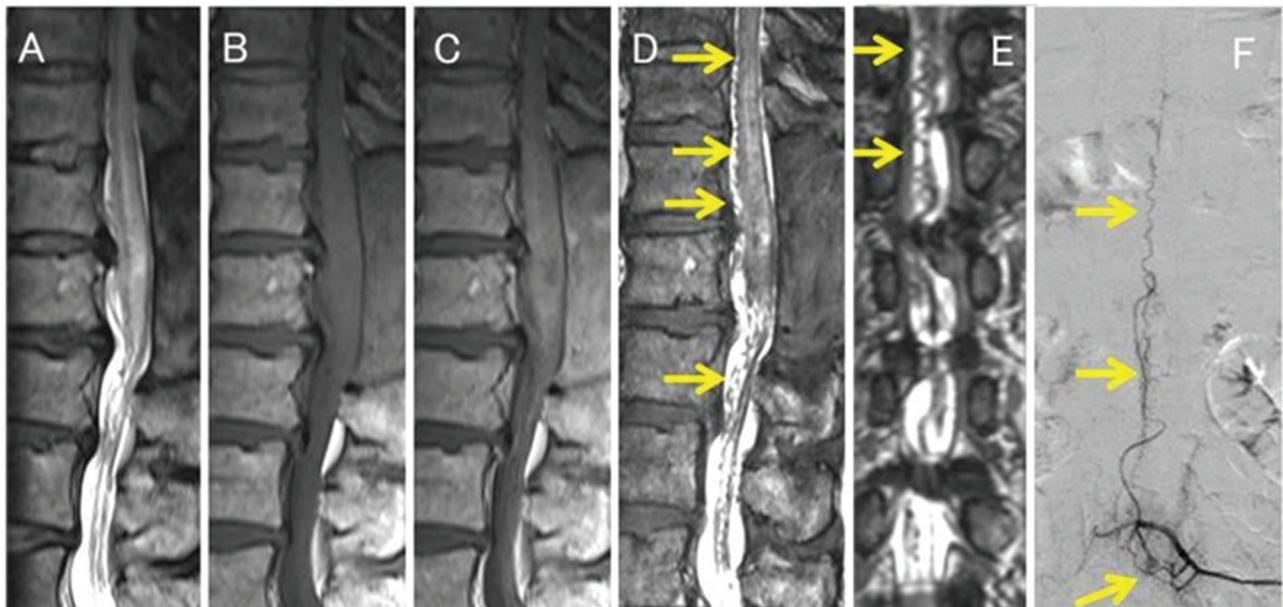


Fig. 1 A 58-year-old man (Case 9) with a spinal dural arteriovenous fistula (SDAVF). Conventional, including sagittal T_2 -weighted (T_2 WI) (A), T_1 -weighted (B), and contrast-enhanced T_1 -weighted (C) MR imaging shows swelling in the thoracic spinal cord and conus medullaris. T_2 WI scans (A) revealed areas with hyperintensity in the spinal cord. Sagittal and coronal 3D constructive interference in steady state (CISS) imaging (D, E) disclosed a tortuous vascular structures (arrows) along the spinal cord. The SDAVF was diagnosed by intra-arterial digital subtraction angiography (F). The site of the SDAVF was the third lumbar vertebral level (arrow). Both readers judged this as grade 3 on 3D CISS and grade 1 on conventional MR images for the identification of abnormal vessels.

patients with SDAVF. However, if the shunt volume is small, no abnormal vessels may be observed on conventional sequences.^{1,12} In our 3T MRI study, we observed flow voids on 13% of T₁WI- and on 69–81% of T₂WI scans. Krings and Geibprasert¹ suggested that for the identification of abnormal vessels of SDAVF, heavily T₂-weighted sequences were more useful than standard T₂WI scans. Morris et al.⁸ reported three cases in which MRI with 3D CISS and 3D phase-cycled fast imaging employing steady state acquisition (PC-FIESTA) was useful not only for the documentation but also the localization of difficult-to-find SDAVF. To our knowledge, ours is the first systematic comparison of the usefulness of 3D CISS images and conventional MRI for the evaluation of SDAVF.

As the 3D CISS sequence does not require the use of gadolinium-based contrast agents, it avoids the risk for nephrogenic systemic fibrosis.¹³ Suspecting the presence of abnormal vessels associated with SDAVF is important for their early diagnosis and following treatment. As the 3D CISS sequence does not involve contrast media and provides useful information about the presence of abnormal vessels associated with SDAVF, it should be added to routine MR studies for SDAVF screening.

Our study presents several limitations. First, we evaluated only axial and sagittal planes with the SE images. The combination of sagittal, axial, and coronal SE sequences may have resulted in the detection of more abnormal vessels associated with SDAVF; however, it is time-consuming. Thus, we can't use that for whole spine evaluation in patients with SDAVF in the clinical situation. 3D CISS images can be reconstructed in any desired cross-sections and such reconstructions along a curved or tilted section are especially useful in these patients. Second, although contrast-enhanced 3D gradient-echo sequences may be useful for the evaluation of spinal arteriovenous shunt lesions¹⁴, we did not assess them in this study. Further studies are needed to clarify the usefulness of 3D CISS imaging compared with contrast-enhanced 3D gradient-echo sequences. Third, 3D CISS images couldn't assess the intramedullary abnormalities related with SDAVF. SE T₂WI scans can demonstrate intramedullary signal changes of the spinal cord associated with SDAVF. We think that 3D CISS and SE T₂WI sequences are complementary imaging methods for the evaluation of SDAVF. Finally, we evaluated only the patients with SDAVF using conventional sequences and CISS images. Since 3D CISS image has a high sensitivity for detection of small structures surrounded by CSF, it remains the possibility that redundant nerve roots of the cauda equine and mild dilated normal veins are interpreted as tortuous abnormal veins associated SDAVF. We think that it is important to detect intramedullary T₂ hyperintensity and tortuous vessels for diagnosis of SDAVF, therefore the combination coronal reconstruction of 3D CISS and SE T₂WI sequences are useful for the evaluation of SDAVF. Further studies with comparison between patients with SDAVF and spinal canal stenosis are needed to clarify the usefulness of 3D CISS in the clinical setting.

Conclusion

The 3D CISS sequence is useful for evaluating the abnormal vessels of SDAVF and should be added to routine MR examinations in patients suspected of harboring SDAVF.

Conflicts of Interest

The authors declare that they have no conflicts of interest.

References

1. Krings T, Geibprasert S. Spinal dural arteriovenous fistulas. *AJNR Am J Neuroradiol* 2009; 30:639–648.
2. Jellema K, Tijssen CC, van Gijn J. Spinal dural arteriovenous fistulas: a congestive myelopathy that initially mimics a peripheral nerve disorder. *Brain* 2006; 129:3150–3164.
3. Cenzato M, Versari P, Righi C, Simionato F, Casali C, Giovanelli M. Spinal dural arteriovenous fistulae: analysis of outcome in relation to pretreatment indicators. *Neurosurgery* 2004; 55:815–822; discussion 822–823.
4. Gilbertson JR, Miller GM, Goldman MS, Marsh WR. Spinal dural arteriovenous fistulas: MR and myelographic findings. *AJNR Am J Neuroradiol* 1995; 16:2049–2057.
5. Hurst RW, Grossman RI. Peripheral spinal cord hypointensity on T2-weighted MR images: a reliable imaging sign of venous hypertensive myelopathy. *AJNR Am J Neuroradiol* 2000; 21:781–786.
6. Ramli N, Cooper A, Jaspan T. High resolution CISS imaging of the spine. *Br J Radiol* 2001; 74:862–873.
7. Krings T, Lasjaunias PL, Hans FJ, et al. Imaging in spinal vascular disease. *Neuroimaging Clin N Am* 2007; 17:57–72.
8. Morris JM, Kaufmann TJ, Campeau NG, Cloft HJ, Lanzino G. Volumetric myelographic magnetic resonance imaging to localize difficult-to-find spinal dural arteriovenous fistulas. *J Neurosurg Spine* 2011; 14:398–404.
9. Hirai T, Korogi Y, Shigematsu Y, et al. Evaluation of syringomyelia with three-dimensional constructive interference in a steady state (CISS) sequence. *J Magn Reson Imaging* 2000; 11:120–126.
10. Haacke EM, Wielopolski PA, Tkach JA, Modic MT. Steady-state free precession imaging in the presence of motion: application for improved visualization of the cerebrospinal fluid. *Radiology* 1990; 175:545–552.
11. Toossi S, Josephson SA, Hetts SW, et al. Utility of MRI in spinal arteriovenous fistula. *Neurology* 2012; 79:25–30.
12. Miller TR, Eskey CJ, Mamourian AC. Absence of abnormal vessels in the subarachnoid space on conventional magnetic resonance imaging in patients with spinal dural arteriovenous fistulas. *Neurosurg Focus* 2012; 32:E15.
13. Yang L, Krefling I, Gorovets A, et al. Nephrogenic systemic fibrosis and class labeling of gadolinium-based contrast agents by the food and drug administration. *Radiology* 2012; 265:248–253.
14. Akter M, Hirai T, Kitajima M, et al. Type 1 perimedullary arteriovenous fistula with subarachnoid hemorrhage: utility of contrast-enhanced 3D gradient-echo technique. *Magn Reson Med Sci* 2011; 10:143–147.